

# Parametric Thermal-Hydraulic Studies of HTGR Reactor Vessel System. Consequences on the Structure Lifetime

Shengqiang Li<sup>1)</sup>, T. Cadiou<sup>2)</sup>, Y. Lejeail<sup>2)</sup>, M. T. Cabrillat<sup>2)</sup>

(1. *Institute of Nuclear and New Energy Technology, Tsinghua University, Beijing 100084, China* 2. *CEA Cadarache, DEN/DER/SESI, France*)

**Abstract:** In the framework of Gas Cooled Reactor design assessment, an important point to calculate is the temperature fields on the main structures in nominal and accidental situations in order to determine the consequences on the reactor lifetime. This document presents such thermal-hydraulic and thermal-mechanical studies for the HTGR (High Temperature Gas-cooled Reactor) vessel system in normal operation and pressurized LOFC (Loss Of Forced Coolant) accidents. Thermal-hydraulic calculations address the key issues for pressurized LOFC transients and evaluate the contribution of main design and modeling parameters. These calculations are performed using the CFD (Computational Fluid Dynamics) code STAR-CD.

For these transients where the primary system remains pressurized, it is necessary to carry out mechanical analyses on the structures to assess the damage levels reached.

Sensitivity studies are conducted taking into account different irradiation levels and types of graphite, different assumptions of mass exchanging rate between the stagnant helium beside the vessel and the coolant in the annular channel between core barrel and vessel, and different assumptions regarding the natural convection of helium.

To determine the structure temperatures, the thermal-hydraulic studies show that the conductivity value of graphite reflectors is the main factor for both the normal operation and the accidental situation considered (pressurized LOFC). The thermal-mechanical analyses allow evaluating the consequences of these loading situations for the lifetime assessment of the main metallic structures, namely the core barrel and the pressure vessel. The results obtained show that, for

both structures, the damage levels remain below design limitations.

**Key words:** HTGR, LOFC, CFD, STAR-CD, GCR

## 1. Introduction

The object of this project is to perform the thermal-hydraulic and thermal-mechanical studies on a Gas Cooled Reactor design. The studies will address the main factors for the HTGR (High Temperature Gas-cooled Reactor) design and processing.

This work is based on the data provided in IAEA benchmark, CRP3, 1997<sup>[1]</sup>.

As one of the Generation IV advanced reactors, the HTGR is a new challenge for the reactor design and operation. Its high efficiency and multi-applications are unique; but these advantages can also induce some problems for the materials in the reactor and structure designs. The safety analysis of HTGR should be performed carefully to make sure it will be always under control.

Both the normal operation and pressurized LOFC (Loss Of Forced Coolant) accidents conditions are studied. The aim of these numerical studies is to evaluate the maximum temperature in the core and temperature evolution on all the components in the reactor cavity. Based on the studies for normal condition, sensitivity studies are also performed. In the LOFC accidents, the reactor is only cooled by the Reactor Cavity Cooling System (RCCS) assuming the Shutdown Cooling System (SCS) and Power Conversion System (PCS) are out of order. The main factors of thermal-hydraulic and thermal-mechanical studies are highlighted; they will be useful for optimizing the future HTGR design.

## 2. Description of Benchmark

The whole Reactor cavity and the components it contains are modeled. The main characteristics are:

- Thermal power: 600 MW
- Helium temperature at the core inlet/outlet: 490 °C/850 °C.
- Helium flow rate through the core: 320 kg/s
- Core coolant pressure: 7 MPa
- Hexagonal shape graphite blocks in the annular core
- The decay heat removal is performed by the RCCS surrounding the

reactor vessel

The transient state studies are based on IAEA benchmark CRP3<sup>[1]</sup>.

Two LOFC accidents are considered for the HTGR in CRP3<sup>[1]</sup>. The first LOFC is accompanied by a rapid depressurization and scram, and cooling behavior by conduction is studied. The second one is a LOFC accompanied by a scram, but without a depressurization. In the present work, we only perform studies on the second LOFC. The objective is to predict the transient reactor vessel temperature, RCCS heat removal rates, and core fuel temperatures throughout the course of accidents.

### 3. Main Assumptions

During the normal operation, the heat is extracted from the core by a forced helium flow and is transferred to the PCS.

In the pressurized LOFC accidents, the coolant flow is progressively decreased and the pressure is maintained at 7 MPa in the core. The PCS and SCS are not operational. The decay heat is removed by passive forms from the core. Radiation, conduction and natural convection are considered in both the reactor vessel and the reactor cavity. The analyses are based on the assumption of a LOFC with pressure in the core. The geometry and physical parameters are consistent with data provided in IAEA-TECDOC-1198 and 1163<sup>[2,3]</sup>.

## 4. Modelling Assumptions

### 4.1 The CFD Analyzing Code

The thermal-hydraulic analyses are processed by Computational Fluid Dynamics (CFD) code STAR-CD<sup>[4,5]</sup>. This general purpose code is used for fluid mechanics and heat transfer calculations. The main characteristics of this software are listed:

- 3 dimensional code
- A finite volume formulation
- Multitype  $k$ - $\epsilon$  model equations supporting for turbulent flow calculations
- Support compressible and incompressible flow calculations
- Support radiation calculation
- Natural convection and Buoyancy-driven flows supporting
- The transport and energy equations for all primary variables, such as

pressure, velocity and temperature

- PISO algorithm for pressure linked equations in transients calculations

#### 4.2 Geometry

The geometry of the studied object is based on the data provided in references [2] and [3]. Tab. 1 sum up the main parameters.

**Tab. 1 Main characteristics of HTGR for normal operation**

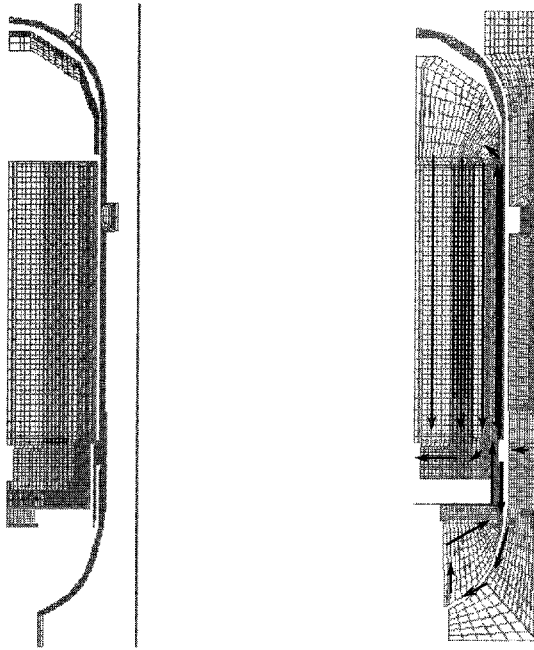
Parameters	Unit	Value
Location	—	Underground containment building
Thermal power	MW	600
Helium temperature at the core inlet	°C	490
Helium temperature at the core outlet	°C	850
Helium flow rate through the core	kg/s	320
Core coolant pressure	MPa	7
Fuel block type	—	Hexagonal
Fuel compact diameter	mm	12.5
Number of fuel blocks	—	102
Number of coolant channels in fuel block	—	108
Core height	m	8
Inner/outer core average diameter	m	2.96/4.84
Vessel outer diameter	m	7.7
Vessel thickness	m	0.2
Coolant channel diameter	mm	16
Hexagonal fuel block width	m	0.36
Refueling interval	d	280
Refueling duration	d	20.7

#### 4.3 Numerical Model

Based on the geometry size described in benchmark, the STAR-CD models are simplified. The PCS and SCS are not described in the models, for the requirement of CPU time. Two 3D models for the HTGR are created with STAR-CD in this work; both models describe reactor cavity system with full scale.

One of two models includes fuel compact, reflectors, hot plenum, core

barrel, duct sleeve, top thermal and neutron shielding, reactor vessel, coolant in the vessel plenum and the channels in the fuel blocks, air in the reactor cavity, RCCS surface cooler near the cavity wall. The other one models all the components above and includes the coolant path in the reflector.



Solid cells of STAR-CD model                      Fluid cells of STAR-CD model  
 Fig. 1 Different types of cell in the model

The 3D models are made in cylindrical coordinate system in radius direction ( $r$ ), circumferential direction ( $\theta$ ), and axial direction ( $z$ ). For CPU time consideration, axis-symmetrical models are used. The models are generated with 5 degrees in the circumferential direction as well as full scalar in other directions. Fig. 1 is side-looking of the 3D model with STAR-CD. In Fig. 1, the coolant path in the reactor vessel during normal operation is shown by black arrows.

The hot duct inlet on the vessel is simplified from an annular channel to a rectangle inlet. The outlet of the hot plenum is also modeled as a rectangle and the hot duct connection structure is ignored. There are 14 869 cells in the CFD model of the HTGR, including 8 078 solid cells, 4 892 fluid cells for coolant in

the vessel system, 1 404 fluid cells for air in the reactor cavity and 495 baffle cells. Fig. 2 is zooming out view of the mesh grid.

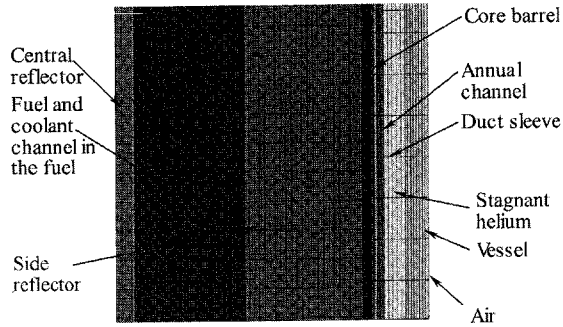


Fig. 2 Zoom out view of models

#### 4.4 Boundary Conditions And Relative Parameters

Core Power distribution and evolution: The core power distribution and evolution during the pressurized LOFC conditions are described. The core power distribution is based on the paper of HTR2002<sup>[6]</sup> as shown in Fig. 3.

The reactor core decay power in the pressurized LOFC is assumed with equation described below ; the decay curve is shown in Fig. 4.

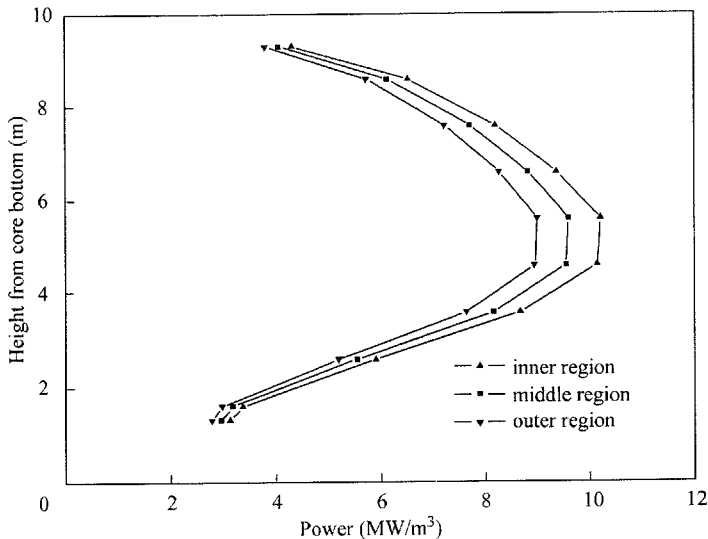


Fig. 3 Power distribution in the core

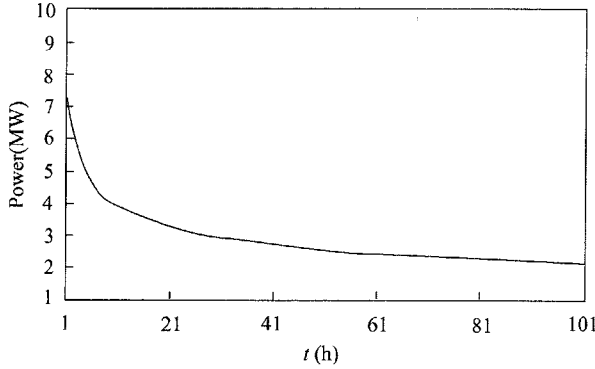


Fig. 4 Decay power evolution

$$P = P_{or} \times (1 - 0.934 \times t) \quad t < 1s \quad (1)$$

$$P = P_{or} \times 0.125 \times t^{-0.28} \quad t \geq 1s \quad (2)$$

$t$ : time (second)

$P$ : decay power on time  $t$  (MW)

$P_{or}$ : thermal power in normal operation (MW)

Materials selection;

- Structure steel: as described in IAEA TECDOC-1198<sup>[2]</sup>, the American steel, 9Cr-1Mo-V, is an alternative steel for the Russian heat resistance steel, 10Cr9MoVNb, with similar level of experience in industry. All the steel structures in the models are assumed to be in 9Cr-1Mo-V. Thermal and mechanical data are taken in RCC-MR<sup>[10]</sup>.
- Helium: all the properties of helium are based on reference[7].
- Air: all the properties of air are based on reference[8].
- Graphite: two types of graphite are considered, one is H451 with a neutron fluence equal to  $7 \times 10^{21}$  n/cm<sup>2</sup>; the other is IG110 moderated by neutron fluence  $2 \times 10^{20}$  n/cm<sup>2</sup>,  $3 \times 10^{20}$  n/cm<sup>2</sup> and  $2.616 \times 10^{22}$  n/cm<sup>2</sup>. For the core is made with graphite and fuel compact, the equivalent conductivity is applied. The parameters of H451 are based on reference [6] while those of IG110 are based on reference [9], [11] and [12]. The irradiation level for normal operation is assumed to be  $2 \times 10^{20}$  n/cm<sup>2</sup>. The data of IG110 for normal operation are shown in Tab. 2 to 4.

**Tab. 2 Conductivity of IG110 under neutron fluence  $2 \times 10^{20}$  n/cm<sup>2</sup>**

T( °C)	500	600	800	1 000	1 200	1 400	1 600
$\lambda_{\text{graphitic}}$ (W/m/K)	67.8	62.4	54.2	49.6	48.7	48.6	48.5
$\lambda_{\text{core}}$ (W/m/K)	39.1	35.9	31.2	28.6	28.1	28.1	28.1

**Tab. 3 Specific heat of graphite and core**

	IG110	Core
$C_p$ (J/kg/K)	1 820	1 840

**Tab. 4 Density of graphite and core**

	IG110	Core
$\rho$ (kg/m <sup>3</sup> )	1 780	1 740

Equivalent conductivity: In reference [2], the core is made of 108 coolant channels in type-1 fuel assembly and 89 coolant channels in type -2 fuel assemblies. As there are many holes inside the fuel block for the coolant channels, the heat exchanging area on the fuel assemblies are much bigger in reality than in the models. To correct the surface area difference, equivalent conductivity and heat transfer coefficient are used.

For calculation, the energy equation is described

$$Q = (T_s - T_w) \times \lambda_s \times S/L_s = S \times h \times (T_w - T_f) \quad (3)$$

Q: heat flux

$T_s$ : temperature in solid

$T_w$ : temperature on the heat exchanging interface

$T_f$ : temperature in fluid

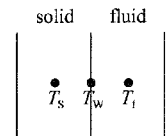
$\lambda_s$ : conductivity of solid

S: heat exchanging surface area

$L_s$ : distance between the temperature referent spot in solid to heat exchanging surface

$h$ : heat transfer coefficient in fluid

The correction will make the heat transfer in the model to be the same value as in the reactor core. The equivalent conductivity and heat transfer coefficient are described with the formulation below.





$$\lambda_m = \lambda_r (S_r L_m / S_m L_r) \quad (4)$$

$$h_m = h_r (S_r / S_m) \quad (5)$$

$\lambda_m$ : conductivity in model

$\lambda_r$ : conductivity in reactor core

$S_r$ : heat transfer area in reactor core

$S_m$ : heat transfer area in model

$L_m$ : distance between temperature reference spot in solid to heat exchanging surface in model

$L_r$ : distance between temperature reference spot in solid to heat exchanging surface in reactor core

$h_r$ : heat transfer coefficient in fluid in reactor core

$h_m$ : heat transfer coefficient in fluid in model

Gap size: the core is constructed with hexagonal fuel and reflector blocks. For the necessity of arrangement of those blocks and specially due to the thermal expansion of graphite and to the volume change under irradiation, gaps exist between those fuel and reflector blocks. Based on the thermal expansion data with fluence<sup>[9]</sup>, estimations for the graphite blocks are made. The variation in radius direction is assessed to 1.2 mm. Assuming an initial gap for arrangement of 1mm, the gap size applied in calculation is 2.2 mm.

Stagnant Helium: as a thin plate, duct sleeve is not the pressure boundary in the vessel, there should be mass exchanging between the two sides of duct sleeve (Fig. 2). In the reference case, we assume that the helium inside the gap between duct sleeve and vessel is not stagnant, but that there are small holes in the duct sleeve leading to a mass exchanging rate of 15% between the He on its two sides. A sensitivity study to the He state in this area will be performed.

RCCS: The RCCS surface cooler are modeled by a wall with fixed temperature on the inside cavity wall. The energy emitted from the vessel system will be transferred to RCCS by radiation, conduction and convection with the air inside the reactor cavity.

Considering the exterior temperature at about 30 °C and the efficiency of water cooler, the inlet water temperature at the bottom of RCCS surface cooler is set to 35 °C.

Boundary conditions:

- Inlet : The inlet parameter of vessel system are shown in Tab. 5. Scram

is happening at the beginning time of pressurized LOFC, the velocity decreasing during the scram stage is described by equation shown below:

$$V = \frac{V_0}{1 + t/6.6} \quad (6)$$

$V$ : m/s

$t$ : s

**Tab. 5 Parameters of inlet**

Material	Helium
Temperature (°C)	490
Mass flux (kg/s)	320

- Outlet ; the boundary condition at the outlet is a constant pressure. The static pressure is 7 MPa.
- Emissivity ; Radiation is active in all fluid regions. The surface emissivity of the interface of solid and fluid region is constant value. The values of emissivity are shown in Tab. 6.

**Tab. 6 Boundary emissivity setting**

Surface	Emissivity	Reflectivity
Core and reflector	0.9	0.1
Top thermal shielding	0.9	0.1
Steel structures	0.8	0.2
Adiabatic boundaries	0.8	0.2

#### 4.5 Meshing

For coolant channel in the fuel and reflector blocks, the honeycomb shape channels in the reality are replaced by an equivalent channel in STAR-CD 3D models. In the fuel blocks, replaceable central reflector blocks and side reflector blocks are represented by an equivalent channel modeled in STAR-CD for each region. There is no mass exchanging between those equivalent channels.

The flow channel local pressure drop for inlet and outlet of hot-duct, annular channel beside core barrel, honeycomb shape channels in the top reflector, fuel blocks and bottom reflector, gap in the central reflector and side

reflector are modeled by baffles.

## **5. Results of Thermal-Hydraulic Studies**

### **5.1 Normal Operation**

The maximum temperature in the core is 1 046.23 °C. The helium average temperature at the outlet is 847.13 °C and the maximum helium temperature is 962.23 °C. The maximum temperature in the graphite reflector is 944.64 °C. The maximum temperature on the vessel is 489.1 °C, it is located on the core supporter part and the inner part of the flange. The maximum temperature in the other parts of vessel is 478.85 °C. These results are pretty higher than those in reference [6]. The explanations of the results are linked to the hypothesis considered for the helium inside the gap between duct sleeve and vessel. As we assume that there is mass exchanging between stagnant helium regions and annular channel, the heat transfer is enhanced by convection. More energy is transferred to outside which gives higher temperature on the vessel and lower temperature in the core.

The maximum velocity of helium is 43.93 m/s as well as the maximum velocity of air is 0.58 m/s.

The pressure drop in the core is 0.51 bar (1 bar =  $10^5$  Pa) while the total pressure drop in the vessel is 0.8 bar.

### **5.2 Sensitivity Studies For Normal Operation**

The sensitivity studies for normal operation include 3 parts - graphite irradiation level, different types of graphite and hypotheses on the state of helium located between the duct sleeve and the annular channel.

- Irradiation level: the influence of the level of neutron flux on the graphite structures behavior is considered. The graphite components are assumed to be in IG 110, three different irradiation levels mentioned in 4.4 are considered.

The conductivity of graphite will change under different irradiation levels while other parameters, such as density, have comparatively low impact. So the different irradiation level will lead to different conductivity in the core. The reference [9], [11] and [12] has shown the relationship between irradiation level and conductivity for graphite IG110.

The temperature results show that high level irradiation on the graphite will evidently increase the maximum temperature in the fuel compact due to a lower heat transfer coefficient between fuel compact and coolant. At the same time, the maximum temperature of reflector will also increase.

The maximum velocity of the coolant increases with the irradiation level increases due to the core temperature increasing. The maximum velocity of air in cavity also increases by a higher irradiation level because larger temperature gradient in the air between the top and the bottom of reactor cavity. The reason of the phenomenon can be explained as below: The temperature on the surface of bottom plenum of vessel are similar in all the cases, it is not affected by conductivity of reflector. But with higher irradiation level side reflector, the vessel surface at middle level of the core will have higher temperature and the increased gradient between them will provide bigger buoyancy force for the air in the reactor cavity.

The RCCS heat removal rate decreases due to low heat flux passing through the reflector to the vessel and the lower temperature on the outside surface of the vessel; furthermore have result as the decrease heat transfer out by radiation.

- Different types of graphite : For different types of graphite, such as IG 110 and H 451, the conductivity evolution curve by temperature will have quite different shape. We select the IG 110 moderated by  $3 \times 10^{20}$  n/cm<sup>2</sup> and H 451 moderated by  $7 \times 10^{21}$  n/cm<sup>2</sup> because the evolution curves of those two graphite have a cross point at about 1150 °C (Fig. 5). The reflector with H 451 has higher maximum temperature and lower average temperature. The maximum temperature is higher due to the lower average conductivity of graphite H 451. The lower average temperature on the reflector is generated from the negative temperature gradient of H 451. As the conductivity evolution curve has positive temperature characters, the graphite near the central core will has higher conductivity, which will be benefit for homogenizing the temperature in the core.

The RCCS heat removal rate decreases with H 451 due to lower heat flux

which response to the lower reflector and vessel temperature. The reason for such phenomenon can be summarized as that the absolute value of average conductivity is a more important factor than conductivity evolution character.

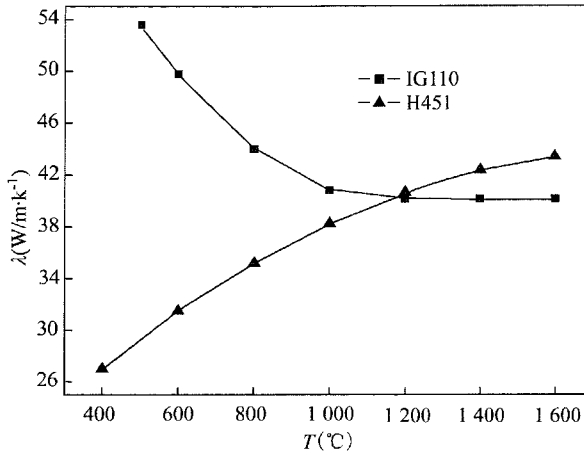


Fig. 5 Conductivity of different types of graphite

- Stagnant helium; This sensitivity study is made for finding out the effect of different mass exchanging rates of stagnant helium between duct sleeve and annular channel.

Two assumptions for the helium between the duct sleeve and vessel are applied. In one case, it assumes that there is no mass exchanging between helium in channel and helium in the annular channel. The natural convection, radiation and conduction are taken into account for stagnant helium. In the other case, there are small holes on the duct sleeve and the mass exchanging rate between the helium on two sides is 15%. The maximum temperature in the core is 0.4 °C higher for the no mass exchange case. The RCCS heat removal rate strongly depends on the vessel and air temperature. The RCCS maximum temperature does not change much because helium in the annular channel is a good thermal shielding to prevent more heat to be lost from the core. The much higher RCCS heat removal rate increases with higher mass exchanging rate due to the helium convection between the two sides.

### 5.3 Pressurized LOFC

The PCS and SCS are assumed both losing efficiency in the LOFC accidents. The initial temperature distribution is based on the data gotten in normal operation studies.

The maximum temperature in the core is shown in Fig. 6. The maximum temperature reaches 1 136.14 °C after 36.25 hours.

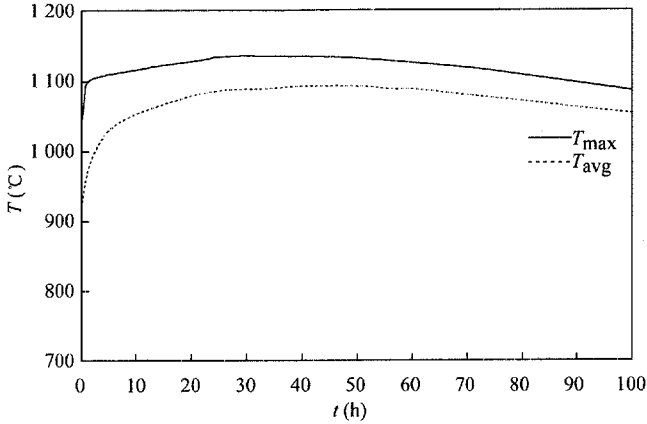


Fig. 6 Maximum and average temperatures in the core

The temperature evolvment curves by time of graphite reflector, core barrier and pressure vessel are shown in Fig. 7.

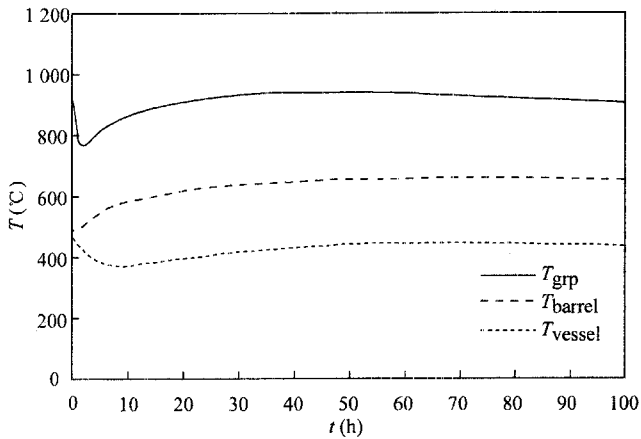


Fig. 7 Reflector graphite and steel structure temperature

Fig. 8 shows the decay power and RCCS heat removal vs time curves and Fig. 9 shows the proportion of conduction and convection contribution in RCCS heat removal.

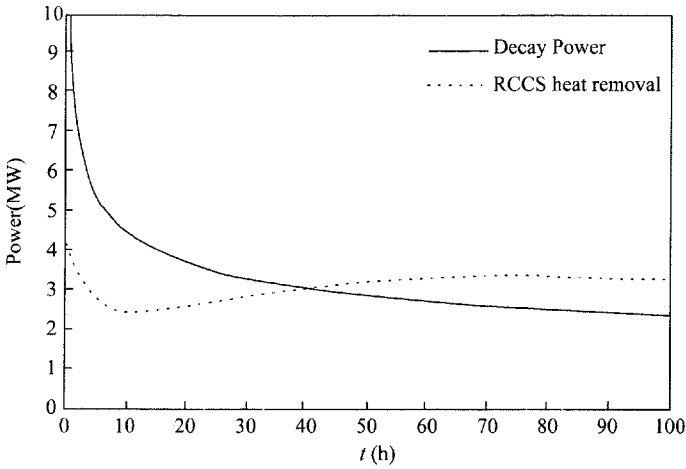


Fig. 8 RCCS and decay heat evolvement curves

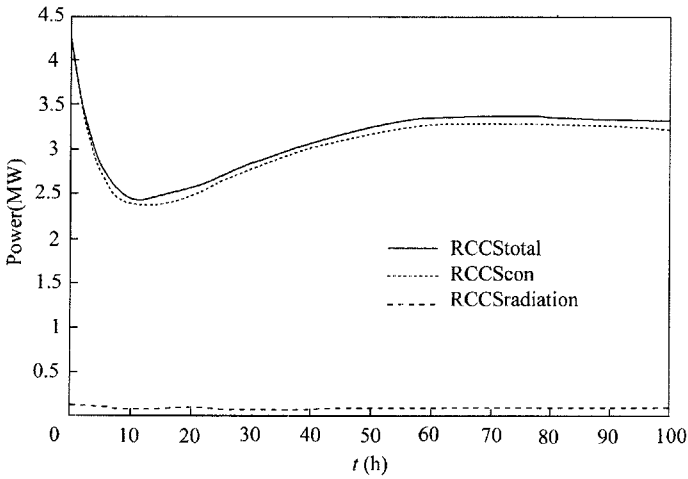


Fig. 9 Conduction/convection and radiation contribution in RCCS heat removal

Temperature distributions of the core along the height at radius 1.72 m are given in Fig. 10.

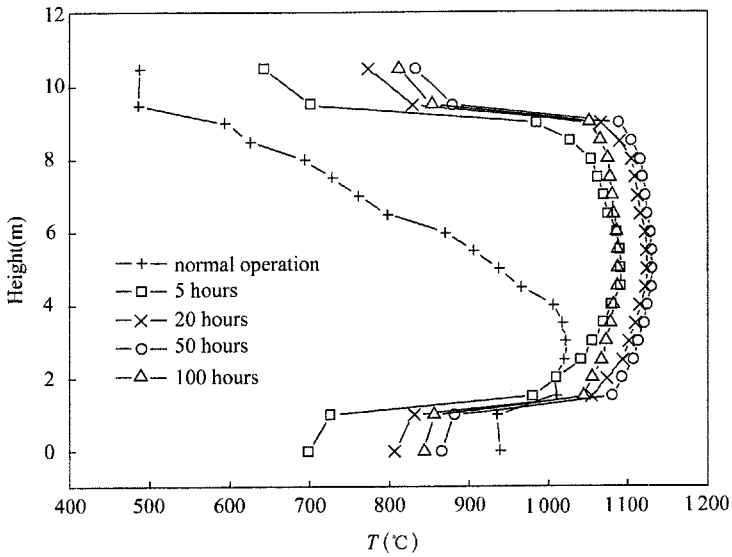


Fig. 10 Axial temperature distribution of core fuel and graphite reflector at radius 1.72 m

Temperature distribution of the core for radius at mid-plane of core is shown in Fig. 11.

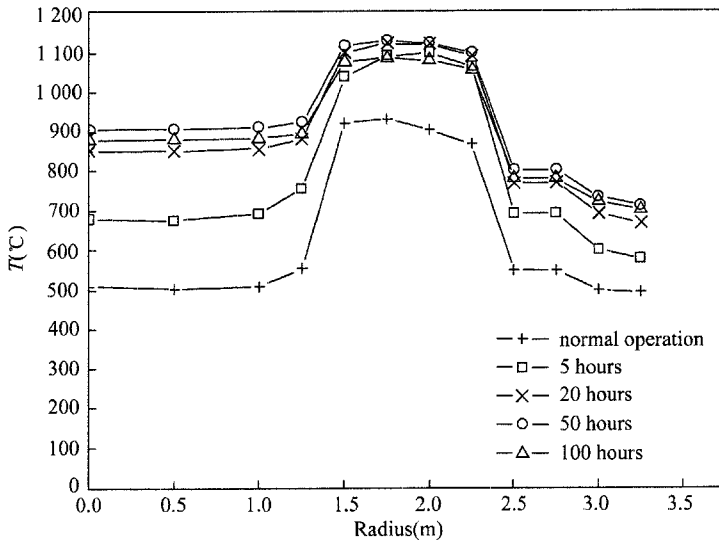


Fig. 11 Radius temperature distribution of core fuel and graphite reflector at mid-plane of core



Temperature of pressure vessel along height is presented in Fig. 12.

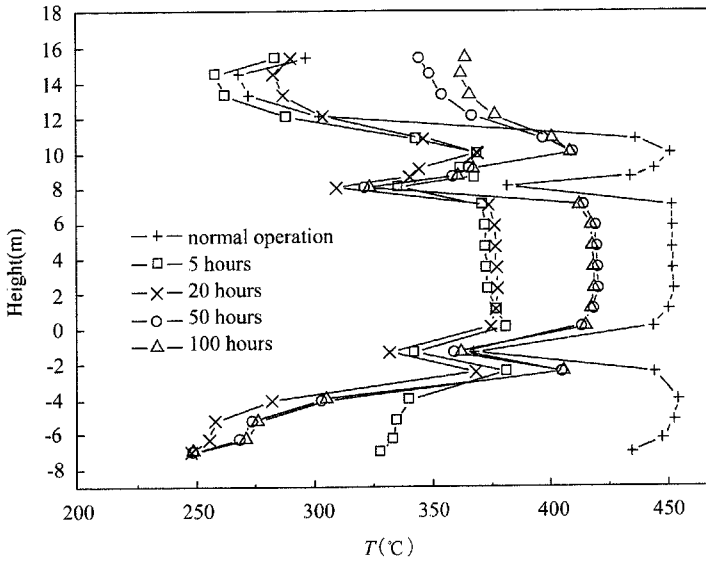


Fig. 12 Vessel temperature distributions along height

The comparison between these studies and reference [3] are made. The results are shown in Tab. 7.

Tab. 7 Comparison of pressurized LOFC

Case	Country	$T_{\text{fuel Max}}(^{\circ}\text{C})$	$t(\text{h})$	$T_{\text{vessel Max}}(^{\circ}\text{C})$	$t(\text{h})$
IAEA-1163	China	1 379	71	370	90
	Netherlands	1 256	8	407	75
	Russia	1 325	65	345	80
	US	980	1	553	48
These cases	With first hour	1 136	36	469	1
	No first hour	1 136	36	437	81

The results show a classical rule: if the core reaches higher temperature, then the time of the peak value will be delayed.

An explanation for the comparison results can be described as below:

The maximum temperature in the core depends on the core conductivity value and distribution in the core; the RCCS heat removal influence is the second factor. That can be also proved by sensitivity studies below.

The results in Tab. 7 also show that the maximum vessel temperature is different from the CRP-3 studies if the first hour in the LOFC is considered. If the first hour result is ignored, then the maximum vessel value is similar to IAEA results.

The explanation is as follows: in these studies, the stagnant helium has strong influence on the normal operation condition and the first stage of pressurized LOFC conditions because if consider of the convection between it and helium in the annular channel, it will enhance the heat transfer from the core to RCCS; otherwise it is a good insulation layer for the vessel. The comparatively low vessel temperature during LOFC is another reason for weaken convection and low heat transfer quantities. Beside of that, the RCCS heat removal rate only depends on the maximum vessel temperature directly but is affected by natural convection in the cavity. That means the RCCS efficiency effect for maximum temperature in the core is low.

Sensitivity studies for pressurized LOFC:

Six types of sensitivity studies are made for pressurized LOFC. They involve the effect of irradiation level, stagnant helium, gap helium, different types of graphite, decay power and natural convection.

Some conclusions can be generated from the sensitivity analyses above which are shown as below.

- The main factor for the maximum fuel temperature is the conductivity of graphite.
- The main factors for RCCS heat removal rate are natural convection, residual power and conductivity of graphite.
- The stagnant helium exchanging rate which has big influence on the RCCS efficiency for normal operation and has smaller influence for LOFC.
- Different types of graphite cases reach peak core temperature at different time but similar value for maximum temperature.
- Reflector graphite is helpful for keeping fuel temperature at a low value by storing residual energy, while reflector temperature is increasing.

- Natural convection of helium in the core will transfer the energy generated in the middle core to top part. Compared with the cases which assume there is no natural convection for the helium in the core, it will decrease the maximum fuel temperature about 89 °C and increase the maximum top thermal temperature about 50 °C.

## 6. Results of Thermal-Mechanical Studies

Mechanical calculations are made to check out the steel structures damage level. All the calculations are based on RCC-MR RB3000<sup>[10]</sup>. The loadings are assumed to be only due to the internal pressure and to the radial thermal gradients in the thickness of the structures studied.

The pressure is kept at 7 MPa for pressurized LOFC and the thermal calculations are based on the temperature calculated by thermohydraulic calculations. Only the mid-plane level part of steel structures is estimated because this region normally has biggest heat flux. The duration of one cycle is 300.7 days, including 280 days for refueling interval and 20.7 days for refueling duration. The reactor life time is considered as 60 years. Consequently a number of around 60 fuel cycles can be estimated for the total life of the reactor.

Creep-fatigue damages are evaluated only for normal operation. It will be necessary in the future to perform creep-fatigue analyses in some transient situations, but for that it will be necessary to have more detailed evaluation of temperature evolution on the structures. Moreover, LOFC is an accidental situations, it will happen only once in the life of the reactor. In these conditions, there is no need to perform fatigue analysis.

With these assumptions, the creep-fatigue damage estimated on the core barrel in normal situations is very low, due to the fact that there is no stress due to pressure and very low thermal gradient in the thickness in all situations.

Concerning the reactor vessel, as the assumption of mass exchanging exist for stagnant helium in our studies; it will make the vessel work in the situation that the creep is not negligible. So the follow calculations are performed as some case studies. For reactor vessel, the thermal gradient is higher. It reaches a maximum value of 53 °C, with an inner temperature of the vessel equal to 478 °C. Theses values are obtained in the reference case and in all sensitivity cases studied except the case corresponding to the hypothesis of a stagnant He

between the duct shell and the vessel. In this last case the thermal gradient is equal to 35 °C, and the inner temperature of the vessel is lower.

For the creep-fatigue analysis, we take into account the thermal gradient and the stresses due to internal pressure. This combination of loadings leads to low equivalent stresses on the inner skin of the vessel (thermal stresses are compressive while stresses due to pressure are tensile), and to higher stresses on the outer skin.

The stress evaluated on the inner skin is equal to 70 MPa. Creep-fatigue analysis leads to very low creep-fatigue damage; more than 105 cycles are allowed. On the outer skin, the stress is evaluated to 200 MPa. With a temperature which is around 425 °C, that leads to more than 104 cycles. As these number of cycles are higher than 60, the creep-fatigue damage on the pressure vessel should be negligible.

Nevertheless, it must be pointed out that some improvements could be done in the model in order to take into account the axial thermal gradients on the structures, the presence of weldments, and the different transients during the life.

## **7. Conclusions**

From the results of thermohydraulic calculations, we can find out that conductivity of graphite in the core will be the most important factor for reactor temperature in normal operation conditions. The absolute value of it will have remarkable influence on maximum temperature in the core as well the graphite conductivity evolution by temperature will change the temperature distribution in the. Beside of that, it will also have influence on the temperature distribution of reactor structure components. Lower conductivity will always give the lower temperature gradient on structures which will relate to lower thermal stress on them. The results of studies show that comparative higher conductivity and positive conductivity evolution characteristic (conductivity increase with temperature increasing) will be benefit for the reactor safety frame as well as they will decrease the operation efficient.

The states of helium between the duct sleeve and reactor vessel is another important factor for the temperature on the vessel while it will not have visible influence on the maximum core temperature. If there is enhanced mass exchange

between the stagnant helium and helium in the annular channel, the maximum temperature gradient on the vessel will increase rapidly. Consider of the mass exchanging for stagnant helium, the negligible creep rule for the pressure vessel will not surely to be satisfied as it will be in no mass exchanging cases. The parametric studies show that even with mass exchanging influence, the reactor vessel will still under design limitations and that is also true for all other parametric calculations. The temperature gradient does not lead the reactor vessel over the design limitation.

The natural convection will change the temperature distribution in the core and on the structures. Consequently, it will have influence on the frame of lower maximum temperature in the core and on the structures.

By our simplified analyses, the natural convection is the most important factor for loading on the steel structures during pressurized LOFC.

As we use the assumption of isotropic conductivity for the graphite reflector, all the studies have not considered of the conductivity difference between axial direction and radius direction. So some further works maybe done for that to study the influence of orthotropic heat transfer in the graphite reflector.

For all the cases, simplified analyses show that the damage levels on the structures are under design limitation. Complementary analyses will be necessary to obtain more precisely the stress in the structures, taking into account the different loadings, the presence of weldments and the different transients during the life of the reactor.

## Note

This work was performed by Dr. Shengqiang Li during his visit in CEA (Cadarache) from November, 2003 to April, 2005.

## References

- [1] S. J. Ball. Submittal for description of GT-MHR plutonium burner benchmark [R]. Oak Ridge National Laboratory Letter, February 11, 97, CRP-3 TECDOC.
- [2] IAEA TECDOC-1198. Current status and future development of modular high temperature gas cooled reactor technology[S]. IAEA, 2001.
- [3] IAEA TECDOE-1163. Heat transport and afterheat removal for gas cooled reactors under

- accident conditions[S]. IAEA, 2000.
- [4] Version 3.15. STAR-CD user guide[S]. Computational Dynamics Limited, 2001.
  - [5] Version 3.15. STAR-CD methodology[S]. Computational Dynamics Limited, 2001.
  - [6] A. Woaye-Hune, S. Ehster. Calculation of decay heat removal transient by passive means for a direct cycle modular HTR[R]. HTR2002, Framatome ANP, 2002.
  - [7] Raymond DRUT. Caractéristiques thermodynamiques de l'hélium: formules et tables, accident, CEA-R-3791[S]. CEA, 1969.
  - [8] Propriété physiques de l'air à l'état gazeux, recommandation n°15 mars 1978[S], DRNR-STRS, CEA, 1978.
  - [9] S. Ishiyama, T. D. Burchell, J. P. Strizak, et al. The effect of high fluence neutron irradiation on the properties of a fine-grained isotropic nuclear graphite[J]. Journal of Nuclear Materials, 1996, 230;1-7.
  - [10] Edition 2002, RCC-MR[S]. CEA, France, 2002.
  - [11] S. Ishiyama, T. D. Burchell, J. P. Strizak, et al. The effect of high fluence neutron irradiation on the properties of a fine-grained isotropic nuclear graphite[J]. Journal of Nuclear Materials, 1996, 230;1-7.
  - [12] T. Oku, M. Ishihara. Lifetime evaluation of graphite components for HTGRs [J]. Nuclear Engineering and Design, 2004, 227;209-217.